Carbon Nanotubes: Present and Future Commercial Applications

Michael F. L. De Volder,[1,2,3]* Sameh H. Tawfick,[4,5] Ray H. Baughman,[6] A. John Hart[4,5]*

Worldwide commercial interest in carbon nanotubes (CNTs) is reflected in a production capacity that presently exceeds several thousand tons per year. Currently, bulk CNT powders are incorporated in diverse commercial products ranging from rechargeable batteries, automotive parts, and sporting goods to boat hulls and water filters. Advances in CNT synthesis, purification, and chemical modification are enabling integration of CNTs in thin-film electronics and large-area coatings. Although not yet providing compelling mechanical strength or electrical or thermal conductivities for many applications, CNT yarns and sheets already have promising performance for applications including supercapacitors, actuators, and lightweight electromagnetic shields.

Carbon nanotubes (CNTs) are seamless cylinders of one or more layers of graphene (denoted single-wall, SWNT, or multiwall, MWNT), with open or closed ends (*1*, *2*). Perfect CNTs have all carbons bonded in a hexagonal lattice except at their ends, whereas defects in mass-produced CNTs introduce pentagons, heptagons, and other imperfections in the sidewalls that generally degrade desired properties. Diameters of SWNTs and MWNTs are typically 0.8 to 2 nm and 5 to 20 nm, respectively, although MWNT diameters can exceed 100 nm. CNT lengths range from less than 100 nm to several centimeters, thereby bridging molecular and macroscopic scales.

When considering the cross-sectional area of the CNT walls only, an elastic modulus approaching 1 TPa and a tensile strength of 100 GPa has been measured for individual MWNTs (*3*). This strength is over 10-fold higher than any industrial fiber. MWNTs are typically metallic and can carry currents of up to 10^9 A cm^{-2} (*4*). Individual CNT walls can be metallic or semiconducting depending on the orientation of the graphene lattice with respect to the tube axis, which is called the chirality. Individual SWNTs can have a thermal conductivity of 3500 W m^{-1} K^{-1} at room temperature, based on the wall area (*5*); this exceeds the thermal conductivity of diamond.

The beginning of widespread CNT research in the early 1990s was preceded in the 1980s by the first industrial synthesis of what are now known as MWNTs and documented observations of hollow carbon nanofibers as early as the 1950s. However, CNT-related commercial activity has grown most substantially during the past decade. Since 2006, worldwide CNT production capacity has increased at least 10-fold, and the annual number of CNT-related journal publications and issued patents continues to grow (Fig. 1).

[1]imec, 3001 Heverlee, Belgium. [2]Department of Mechanical Engineering, KULeuven, 3000 Leuven, Belgium. [3]School of Engineering and Applied Sciences, Harvard University, Cambridge, MA 02138, USA. [4]Department of Mechanical Engineering, University of Michigan, Ann Arbor, MI 48109, USA. [5]Department of Mechanical Engineering, Massachusetts Institute of Technology, Cambridge, MA 02139, USA. [6]The Alan G. MacDiarmid NanoTech Institute and Department of Chemistry, University of Texas at Dallas, Richardson, TX 75083, USA.

*To whom correspondence should be addressed. E-mail: michael.devolder@imec.be (M.F.L.D.V.); ajohnh@umich.edu (A.J.H.)

Most CNT production today is used in bulk composite materials and thin films, which rely on unorganized CNT architectures having limited properties. Organized CNT architectures (fig. S1) such as vertically aligned forests, yarns, and sheets show promise to scale up the properties of individual CNTs and realize new functionalities, including shape recovery (*6*), dry adhesion (*7*), high damping (*8*, *9*), terahertz polarization (*10*), large-stroke actuation (*11*, *12*), near-ideal black-body absorption (*13*), and thermoacoustic sound emission (*14*).

However, presently realized mechanical, thermal, and electrical properties of CNT macrostructures such as yarns and sheets remain significantly lower than those of individual CNTs.

Meanwhile, buoyed by large-volume bulk production, CNT powders have already been incorporated in many commercial applications and are now entering the growth phase of their product life cycle. In view of these trends, this review focuses on the most promising present and future commercial applications of CNTs, along with related challenges that will drive continued research and development. Lists of known industrial activity and commercial products are given in tables S1 through S3.

CNT Synthesis and Processing

Chemical vapor deposition (CVD) is the dominant mode of high-volume CNT production and typically uses fluidized bed reactors that enable uniform gas diffusion and heat transfer to metal catalyst nanoparticles (*15*). Scale-up, use of low-cost feedstocks, yield increases, and reduction of energy consumption and waste production (*16*) have substantially decreased MWNT prices. However, large-scale CVD methods yield contaminants that can influence CNT properties and often require costly thermal annealing and/or chemical treatment for their removal. These steps can introduce defects in CNT sidewalls and shorten CNT length. Currently, bulk purified MWNTs are sold for less than $100 per kg, which is 1- to 10-fold greater than commercially available carbon fiber.

The understanding of CVD process conditions has enabled preferential synthesis of metallic (*17*) or semiconducting SWNTs (*18*) with selectivity of 90 to 95%, doping of CNTs with boron or nitrogen

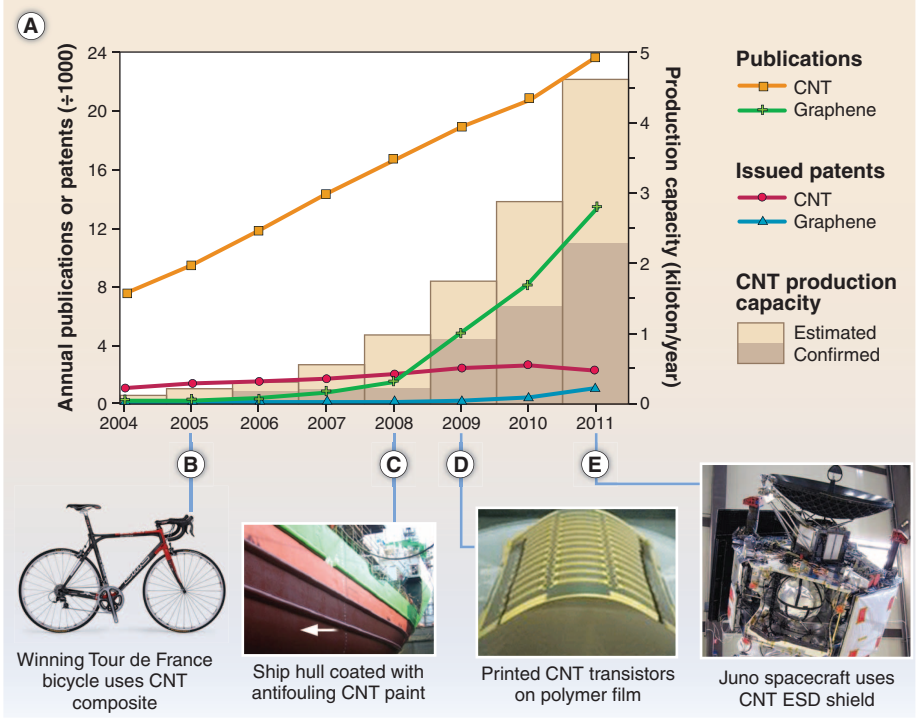

Fig. 1. Trends in CNT research and commercialization. (**A**) Journal publications and issued worldwide patents per year, along with estimated annual production capacity (see supplementary materials). (**B** to **E**) Selected CNT-related products: composite bicycle frame [Photo courtesy of BMC Switzerland AG], antifouling coatings [Courtesy of NanoCyl], printed electronics [Photo courtesy of NEC Corporation; unauthorized use not permitted]; and electrostatic discharge shielding [Photo courtesy of NanoComp Technologies, Incorporated].

(*19*, *20*), and flow-directed growth of isolated SWNTs up to 18.5 cm long (*21*). However, improved knowledge is urgently needed of how CNT chirality, diameter, length, and purity relate to catalyst composition and process conditions. In situ observation of CNT nucleation (*22*) and molecular modeling of the CNT-catalyst interface (*23*) will be critical to advances in chirality-selective synthesis.

Alternatively, high-purity SWNT powders can be separated according to chirality by density-gradient centrifugation in combination with selective surfactant wrapping (*24*) or by gel chromatography (*25*). Although many CNT powders and suspensions are available commercially, the production of stable CNT suspensions requires chemical modification of the CNT surface or addition of surfactants. Washing or thermal treatment is typically needed to remove surfactants after deposition of the solution, such as by spin-coating or printing.

Moreover, because SWNT synthesis by CVD requires much tighter process control than MWNT synthesis and because of legacy costs of research and process development, bulk SWNT prices are still orders of magnitude higher than for MWNTs. Use of MWNTs is therefore favored for applications where CNT diameter or bandgap is not critical, but most emerging applications that require chirality-specific SWNTs need further price reduction for commercial viability.

Alternatively, synthesis of long, aligned CNTs that can be processed without the need for dispersion in a liquid offers promise for cost-effective realization of compelling bulk properties. These methods include self-aligned growth of horizontal (*26*) and vertical (*27*) CNTs on substrates coated with catalyst particles and production of CNT sheets and yarns directly from floating-catalyst CVD systems (*28*). CNT forests can be manipulated into dense solids (*29*), aligned thin films (*30*), and intricate three-dimensional (3D) microarchitectures (*31*) and can be directly spun or drawn into long yarns and sheets (*32*, *33*).

Composite Materials

MWNTs were first used as electrically conductive fillers in plastics, taking advantage of their high aspect ratio to form a percolation network at concentrations as low as 0.01 weight percent (wt %). Disordered MWNT-polymer composites reach conductivities as high as 10,000 S m^{-1} at 10 wt % loading (*34*). In the automotive industry, conductive CNT plastics have enabled electrostatic-assisted painting of mirror housings, as well as fuel lines and filters that dissipate electrostatic charge. Other products include electromagnetic interference (EMI)–shielding packages and wafer carriers for the microelectronics industry.

For load-bearing applications, CNT powders mixed with polymers or precursor resins can increase stiffness, strength, and toughness (*35*). Adding ~1 wt % MWNT to epoxy resin enhances stiffness and fracture toughness by 6 and 23%, respectively, without compromising other mechanical properties (*36*). These enhancements depend on CNT diameter, aspect ratio, alignment, dispersion, and interfacial interaction with the matrix. Many CNT manufacturers sell premixed resins and master batches with CNT loadings from 0.1 to 20 wt %. Additionally, engineering nanoscale stick-slip among CNTs and CNT-polymer contacts can increase material damping (*37*), which is used to enhance sporting goods, including tennis racquets, baseball bats, and bicycle frames (Fig. 1C).

CNT resins are also used to enhance fiber composites (*35*, *38*). Recent examples include strong, lightweight wind turbine blades and hulls for maritime security boats that are made by using carbon fiber composite with CNT-enhanced resin (Fig. 2A) and composite wind turbine blades. CNTs can also be deployed as additives in the organic precursors used to form carbon fibers. The CNTs influence the arrangement of carbon in the pyrolyzed fiber, enabling fabrication of 1-μm diameter carbon fibers with over 35% increase in strength (4.5 GPa) and stiffness (463 GPa) compared with control samples without CNTs (*39*).

Toward the challenge of organizing CNTs at larger scales, hierarchical fiber composites have been created by growing aligned CNTs forests onto glass, SiC, alumina, and carbon fibers (*35*, *40*, *41*), creating so-called "fuzzy" fibers. Fuzzy CNT-SiC fabric impregnated with epoxy showed crack-opening (mode I) and in-plane shear interlaminar (mode II) toughnesses that are enhanced by 348 and 54%, respectively, compared with control specimens (*40*), and CNT-alumina fabric showed 69% improved mode II toughness (*41*). Multifunctional applications under investigation include lightning-strike protection, deicing, and structural health monitoring for aircraft (*35*, *40*).

In the long run, CNT yarns and laminated sheets made by direct CVD or forest spinning or drawing methods may compete with carbon fiber for high-end uses, especially in weight-sensitive applications requiring combined electrical and mechanical functionality (Figs. 1E and 2B). In scientific reports, yarns made from high-quality few-walled CNTs have reached a stiffness of 357 GPa and a strength of 8.8 GPa but only for a gauge length that is comparable to the millimeter-long CNTs within the yarn (*28*). Centimeter-scale gauge lengths showed 2-GPa strength, corresponding to a gravimetric strength equaling that of commercially available Kevlar (DuPont).

Because the probability of a critical flaw increases with volume, macroscale CNT yarns may never achieve the strength of the constituent CNTs. However, the high surface area of CNTs may provide interfacial coupling that mitigates these deficiencies, and, unlike carbon fibers, CNT yarns can be knotted without degrading their strength (*32*). Further, coating forest-drawn CNT sheets with functional powder before inserting twist has provided weavable, braidable, and sewable yarns containing up to 95 wt % powder, which have been demonstrated as superconducting wires, battery and fuel cell electrodes, and self-cleaning textiles (*42*).

High-performance fibers of aligned SWNTs can be made by coagulation-based spinning of CNT suspensions (*43*). This is attractive for scale-up if the cost of high-quality SWNTs decreases substantially or if spinning can be extended to low-cost MWNTs. Thousands of spinnerets could operate in parallel, and CNT orientation can be achieved via liquid crystal formation, like for the spinning of Kevlar.

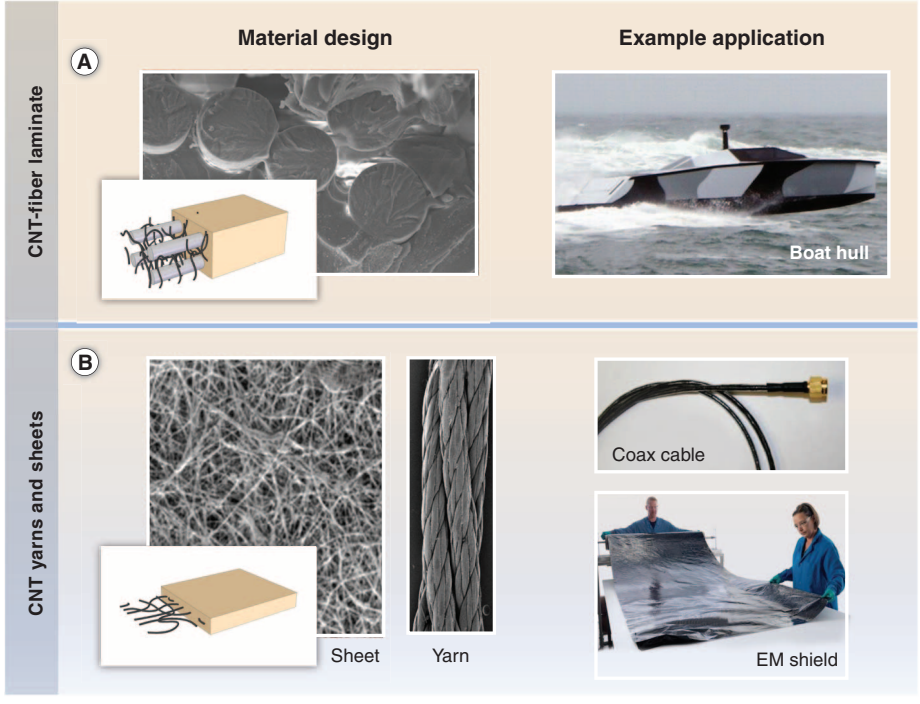

Fig. 2. Emerging CNT composites and macrostructures. **(A)** Micrograph showing the cross section of a carbon fiber laminate with CNTs dispersed in the epoxy resin and a lightweight CNT-fiber composite boat hull for maritime security boats. [Images courtesy of Zyvex Technologies] **(B)** CNT sheets and yarns used as lightweight data cables and electromagnetic (EM) shielding material. [Images courtesy of Nanocomp Technologies, Incorporated]

Besides polymer composites, the addition of small amounts of CNTs to metals has provided increased tensile strength and modulus (*44*) that may find applications in aerospace and automotive structures. Commercial Al-MWNT composites have strengths comparable to stainless steel (0.7 to 1 GPa) at one-third the density (2.6 g cm^{-3}). This strength is also comparable to Al-Li alloys, yet the Al-MWNT composites are reportedly less expensive.

Last, MWNTs can also be used as a flame-retardant additive to plastics; this effect is mainly attributed to changes in rheology by nanotube loading (*45*). These nanotube additives are commercially attractive as a replacement for halogenated flame retardants, which have restricted use because of environmental regulations.

Coatings and Films

Leveraging CNT dispersion, functionalization, and large-area deposition techniques, CNTs are emerging as a multifunctional coating material. For example, MWNT-containing paints reduce biofouling of ship hulls (Fig. 1C) by discouraging attachment of algae and barnacles (*46*). They are a possible alternative to environmentally hazardous biocide-containing paints. Incorporation of CNTs in anticorrosion coatings for metals can enhance coating stiffness and strength while providing an electric pathway for cathodic protection.

Widespread development continues on CNT-based transparent conducting films (*47*) as an alternative to indium tin oxide (ITO). A concern is that ITO is becoming more expensive because of the scarcity of indium, compounded by growing demand for displays, touch-screen devices, and photovoltaics. Besides cost, the flexibility of CNT transparent conductors is a major advantage over brittle ITO coatings for flexible displays. Further, transparent CNT conductors can be deposited from solution (e.g., slot-die coating, ultrasonic spraying) and patterned by cost-effective nonlithographic methods (e.g., screen printing, microplotting). Recent commercial development effort has resulted in SWNT films with 90% transparency and a sheet resistivity of 100 ohm per square. This surface resistivity is adequate for some applications but still substantially higher than for equally transparent, optimally doped ITO coatings (*48*). Related applications that have less stringent requirements include CNT thin-film heaters, such as for defrosting windows or sidewalks. All of the above coatings are being pursued industrially (see table S3).

Microelectronics

High-quality SWNTs are attractive for transistors because of their low electron scattering and their bandgap, which depends on diameter and chiral angle. Further, SWNTs are compatible with field-effect transistor (FET) architectures and high-k dielectrics (*26*, *49*). After the first CNT transistor in 1998 (*50*), milestones include the first SWNT-tunneling FET with a subthreshold swing of <60 mV $decade^{-1}$ in 2004 (*49*, *51*) and CNT-based radios in 2007 (*52*). In 2012, SWNT FETs with sub-10-nm channel lengths showed a normalized current density (2.41 mA μm^{-1} at 0.5 V), which is greater than those obtained for silicon devices (*53*).

Despite the promising performance of individual SWNT devices, control of CNT diameter, chirality, density, and placement remains insufficient for microelectronics production, especially over large areas. Therefore, devices such as transistors comprising patterned films of tens to thousands of SWNTs are more immediately practical. The use of CNT arrays increases output current and compensates for defects and chirality differences, improving device uniformity and reproducibility (*26*). For example, transistors using horizontally aligned CNT arrays achieved mobilities of 80 $cm^2 V^{-1} s^{-1}$, subthreshold slopes of 140 mV $decade^{-1}$, and on/off ratios as high as 10^5 (*54*). These developments are supported by recent methods for precise high-density CNT film deposition methods, enabling conventional semiconductor fabrication of more than 10,000 CNT devices in a single chip (*55*).

CNT thin-film transistors (TFTs) are particularly attractive for driving organic light-emitting diode (OLED) displays, because they have shown higher mobility than amorphous silicon (~1 $cm^2 V^{-1} s^{-1}$) (*56*) and can be deposited by low-temperature, nonvacuum methods. Recently, flexible CNT TFTs with a mobility of 35 $cm^2 V^{-1} s^{-1}$ and an on/off ratio of 6×10^6 were demonstrated (Fig. 3A) (*56*). A vertical CNT FET showed sufficient current output to drive OLEDs at low voltage (*57*), enabling red-green-blue emission by the OLED through a transparent CNT network. Promising commercial development of CNT electronics includes low-cost printing of TFTs (*58*), as well as radio-frequency identification tags (*59*). Improved understanding of CNT surface chemistry is essential for commercialization of CNT thin-film electronics; recent developments enable, for example, selective retention of semiconducting SWNTs during spin-coating (*60*) and reduction of sensitivity to adsorbates (*61*).

The International Technology Roadmap for Semiconductors suggests that CNTs could replace Cu in microelectronic interconnects, owing to their low scattering, high current-carrying capacity, and resistance to electromigration. For this, vias comprising tightly packed (>10^{13} per cm^2) metallic CNTs with low defect density and low contact resistance are needed. Recently, complementary metal oxide semiconductor (CMOS)–compatible 150-nm-diameter interconnects (Fig. 3C) with a single CNT–contact hole resistance of 2.8 kohm were demonstrated on full 200-mm-diameter wafers (*62*). Also, as a replacement for solder bumps, CNTs can function both as electrical leads and heat dissipaters for use in high-power amplifiers (Fig. 3D).

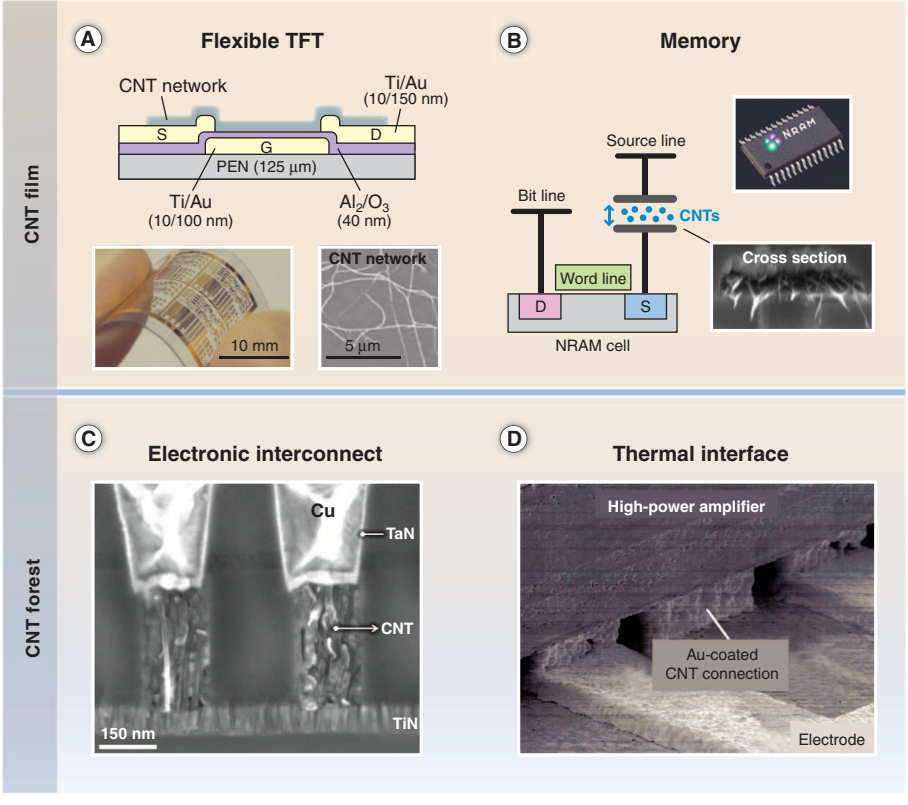

Fig. 3. Selected CNT applications in microelectronics. (**A**) Flexible TFTs using CNT networks deposited by aerosol CVD. [Schematic and photograph reprinted by permission from Macmillan Publishers Limited; scanning electron microscopy image courtesy of Y. Ohno] (**B**) CNT-based nonvolatile random access memory (NRAM) cell fabricated by using spin-coating and patterning of a CMOS-compatible CNT solution. [Images courtesy of Nantero, Incorporated] (**C**) CMOS-compatible 150-nm vertical interconnects developed by imec and Tokyo Electron Limited. [Image courtesy of imec] (**D**) CNT bumps used for enhanced thermal dissipation in high power amplifiers. [Image courtesy of Fujitsu Limited]

Last, a concept for a nonvolatile memory based on individual CNT crossbar electromechanical switches (*63*) has been adapted for commercialization (Fig. 3B) by patterning tangled CNT thin films as the functional elements. This required development of ultrapure CNT suspensions that can be spin-coated and processed in industrial clean room environments and are therefore compatible with CMOS processing standards.

Energy Storage and Environment

MWNTs are widely used in lithium ion batteries for notebook computers and mobile phones, marking a major commercial success (*64*, *65*). In these batteries, small amounts of MWNT powder are blended with active materials and a polymer binder, such as 1 wt % CNT loading in $LiCoO_2$ cathodes and graphite anodes. CNTs provide increased electrical connectivity and mechanical integrity, which enhances rate capability and cycle life (*64*, *66*, *67*).

Many publications report gravimetric energy storage and power densities for unpackaged batteries and supercapacitors, where normalization is with respect to the weight of active electrode materials. The frequent use of low areal densities for active materials makes it difficult to assess how such gravimetric performance metrics relate to those for packaged cells (*68*, *69*), where high areal energy storage and power densities are needed for realizing high performance based on total cell weight or volume. In one of the few recent studies for packaged cells, remarkable performance has been obtained for supercapacitors deploying forest-grown SWNTs (*62*) that are binder and additive free; an energy density of 16 Wh kg^{-1} and a power density of 10 kW kg^{-1} was obtained for a 40-F supercapacitor with a maximum voltage of 3.5 V. On the basis of accelerated tests at up to 105°C, a 16-year lifetime was forecast. Despite these impressive metrics, the present cost of SWNTs is a major roadblock to commercialization.

For fuel cells, the use of CNTs as a catalyst support can potentially reduce Pt usage by 60% compared with carbon black (*70*), and doped CNTs may enable fuel cells that do not require Pt (*19*, *71*). For organic solar cells, ongoing efforts are leveraging the properties of CNTs to reduce undesired carrier recombination and enhance resistance to photooxidation (*20*). In the long run, photovoltaic technologies may incorporate CNT-Si heterojunctions and leverage efficient multiple-exciton generation at p-n junctions formed within individual CNTs (*72*). In the nearer term, commercial photovoltaics may incorporate transparent SWNT electrodes (Fig. 4C).

An upcoming application domain of CNTs is water purification. Here, tangled CNT sheets can provide mechanically and electrochemically robust networks with controlled nanoscale porosity. These have been used to electrochemically oxidize organic contaminants (*73*), bacteria, and viruses (*74*). Portable filters containing CNT meshes have been commercialized for purification of contaminated drinking water (Fig. 4D). Moreover, membranes using aligned encapsulated CNTs with open ends permit flow through the interior of the CNTs, enabling unprecedented low flow resistance for both gases and liquids (*75*). This enhanced permeability may enable lower energy cost for water desalination by reverse osmosis in comparison to commercial polycarbonate membranes. However, very-small-diameter SWNTs are needed to reject salt at seawater concentrations (*76*).

Biotechnology

Ongoing interest in CNTs as components of biosensors and medical devices is motivated by the dimensional and chemical compatibility of CNTs with biomolecules, such as DNA and proteins. At the same time, CNTs enable fluorescent (*77*) and photoacoustic imaging (*78*), as well as localized heating using near-infrared radiation (*79*).

SWNT biosensors can exhibit large changes in electrical impedance (*80*) and optical properties (*81*) in response to the surrounding environment, which is typically modulated by adsorption of a target on the CNT surface. Low detection limits and high selectivity require engineering the CNT surface (e.g., functional groups and coatings) (*80*) and appropriate sensor design (e.g., field effects, capacitance, Raman spectral shifts, and photoluminescence) (*82*, *83*). Products under development include inkjet–printed test strips for estrogen and progesterone detection, microarrays for DNA and protein detection, and sensors for NO_2 and cardiac troponin (*84*). Similar CNT sensors have been used for gas and toxin detection in the food industry, military, and environmental applications (*82*, *85*).

For in vivo applications, CNTs can be internalized by cells, first by binding of their tips to receptors on the cell membrane (*86*). This enables transfection of molecular cargo attached to the CNT walls or encapsulated inside the CNTs (*87*). For example, the cancer drug doxorubicin was loaded at up to 60 wt % on CNTs compared with 8 to 10 wt % on liposomes (*88*). Cargo release can be triggered by using near-infrared radiation. However, for use of free-floating CNTs it will be critical to control the retention of CNTs within the body and prevent undesirable accumulation, which may result from changing CNT surface chemistry (*89*).

Potential CNT toxicity remains a concern, although it is emerging that CNT geometry and surface chemistry strongly influence biocompatibility, and therefore CNT biocompatibility may be engineerable (*89*). Early on, it was reported that injection of large quantities of MWNTs into the lungs of mice could cause asbestos-like pathogenicity (*90*). However, a later study reported that lung inflammation caused by injection of well-dispersed SWNTs was insignificant both compared with asbestos and with particulate matter in air collected in Washington, DC (*91*). Future medical acceptance of CNTs requires deeper understanding of immune response, along with definition of exposure standards for different use cases including inhalation, injection, ingestion, and skin contact. Toward use in implants, CNT forests immobilized in a polymer were studied by implantation into rats and did not show elevated inflammatory

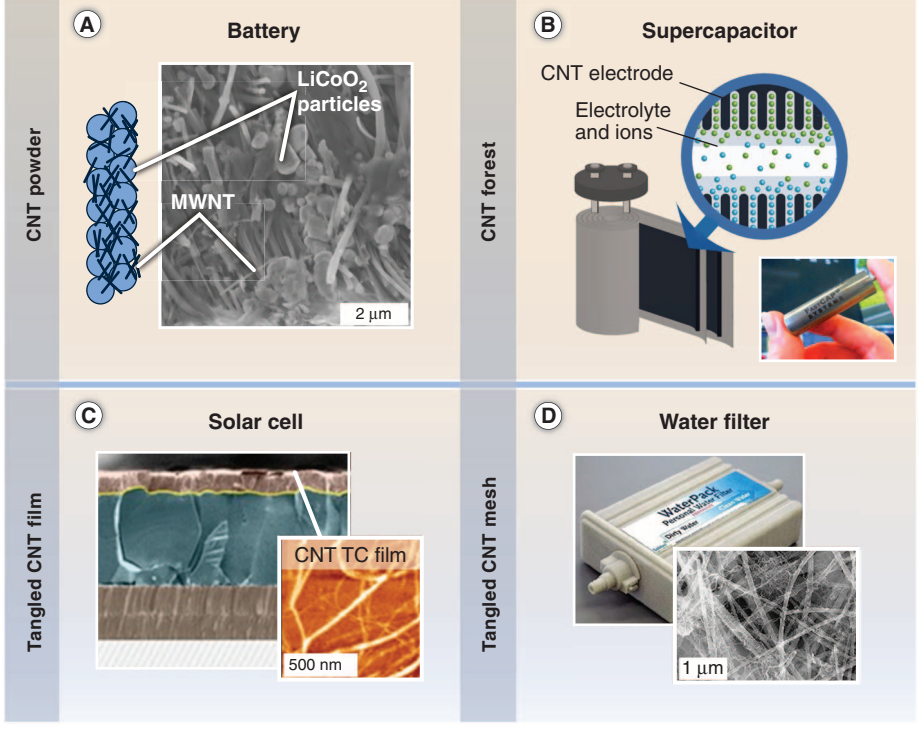

Fig. 4. Energy-related applications of CNTs. (**A**) Mixture of MWNTs and active powder for battery electrode. [Images reprinted by permission from John Wiley and Sons (*67*)] (**B**) Concept for supercapacitors based on CNT forests. [Images courtesy of FastCap Systems Corporation] (**C**) Solar cell using a SWNT-based transparent conductor. [Images courtesy of Eikos Incorporated] (**D**) Prototype portable water filter using a functionalized tangled CNT mesh in the latest stage of development. [Images courtesy of Seldon Technologies]

response relative to controls (*92*). This is encouraging for possible use of CNTs as low-impedance neural interface electrodes (*93*) and for coating of catheters to reduce thrombosis (*94*).

Outlook

Most products using CNTs today incorporate CNT powders dispersed in polymer matrices or deposited as thin films; for commercialization of these products, it was essential to integrate CNT processing with existing manufacturing methods. Organized CNT materials such as forests and yarns are beginning to bridge the gap between the nanoscale properties of CNTs and the length scales of bulk engineering materials. However, understanding is needed of why the properties of CNT yarns and sheets, like thermal conductivity and mechanical strength, remain far lower than the properties of individual CNTs. At an opposite limit, placement of individual CNTs having desired structure with lithographic precision over large substrates would be a breakthrough for electronic devices and scanning probe tips.

According to press reports, many companies are investing in diverse applications of CNTs, such as transparent conductors, thermal interfaces, antiballistic vests, and wind turbine blades. However, often few technical details are released, and companies are likely to keep technical details hidden for a very long time after commercialization, which makes it challenging to predict market success. Hence, the increases in nanotube production capacity and sales are an especially important metric for emerging CNT applications (see Fig. 1).

Further industrial development demands health and safety standards for CNT manufacturing and use, along with improved quantitative characterization methods that can be implemented in production processes. For example, the National Institute of Standards and Technology developed a SWNT reference material in 2011; IEEE is developing standards for CNT processing in clean rooms; and in 2010 the Chinese government published standards for MWNT characterization and handling (*16*). Proactively, Bayer established an occupational exposure limit of 0.05 mg m^{-3} for their CNTs (*95*). These efforts encourage continued progress with caution, especially for CNT manufacturing operations that can potentially generate airborne particulate matter.

As larger quantities of CNT materials reach the consumer market, it will also be necessary to establish disposal and/or reuse procedures. CNTs may enter municipal waste streams, where, unless they are incinerated, cross-contamination during recycling is possible (*65*). Broader partnerships among industry, academia, and government are needed to investigate the environmental and societal impact of CNTs throughout their life cycle.

Lastly, continued CNT research and development will be complementary to the rise of graphene. Rapid innovations in graphene synthesis and characterization—such as CVD methods and Raman spectroscopy techniques—have leveraged findings from CNT research. Promising materials combining carbon allotropes include 3D CNT-graphene networks for thermal interfaces (*96*) and fatigue-resistant graphene-coated CNT aerogels (*97*). The science and applications of CNTs, ranging from surface chemistry to large-scale manufacturing, will contribute to the frontier of nanotechnology and related commercial products for many years to come.

References and Notes

1. S. Iijima, *Nature* **354**, 56 (1991).
2. P. J. F. Harris, *Carbon Nanotube Science - Synthesis, Properties, and Applications* (Cambridge Univ. Press, Cambridge, 2009).
3. B. Peng *et al*., *Nat. Nanotechnol.* **3**, 626 (2008).
4. B. Q. Wei, R. Vajtai, P. M. Ajayan, *Appl. Phys. Lett.* **79**, 1172 (2001).
5. E. Pop, D. Mann, Q. Wang, K. Goodson, H. J. Dai, *Nano Lett.* **6**, 96 (2006).
6. A. Y. Cao, P. L. Dickrell, W. G. Sawyer, M. N. Ghasemi-Nejhad, P. M. Ajayan, *Science* **310**, 1307 (2005).
7. L. Qu, L. Dai, M. Stone, Z. Xia, Z. L. Wang, *Science* **322**, 238 (2008).
8. M. Xu, D. N. Futaba, T. Yamada, M. Yumura, K. Hata, *Science* **330**, 1364 (2010).
9. M. F. L. De Volder, J. De Coster, D. Reynaerts, C. Van Hoof, S.-G. Kim, *Small* **8**, 2006 (2012).
10. L. Ren *et al*., *Nano Lett.* **9**, 2610 (2009).
11. A. E. Aliev *et al*., *Science* **323**, 1575 (2009).
12. M. Lima *et al*., *Science* **338**, 928 (2012).
13. K. Mizuno *et al*., *Proc. Natl. Acad. Sci. U.S.A.* **106**, 6044 (2009).
14. L. Xiao *et al*., *Nano Lett.* **8**, 4539 (2008).
15. M. Endo, T. Hayashi, Y.-A. Kim, *Pure Appl. Chem.* **78**, 1703 (2006).
16. Q. Zhang, J.-Q. Huang, M.-Q. Zhao, W.-Z. Qian, F. Wei, *ChemSusChem* **4**, 864 (2011).
17. A. R. Harutyunyan *et al*., *Science* **326**, 116 (2009).
18. L. Ding *et al*., *Nano Lett.* **9**, 800 (2009).
19. K. Gong, F. Du, Z. Xia, M. Durstock, L. Dai, *Science* **323**, 760 (2009).
20. J. M. Lee *et al*., *Adv. Mater.* **23**, 629 (2011).
21. X. Wang *et al*., *Nano Lett.* **9**, 3137 (2009).
22. S. Hofmann *et al*., *Nano Lett.* **7**, 602 (2007).
23. E. C. Neyts, A. C. T. van Duin, A. Bogaerts, *J. Am. Chem. Soc.* **133**, 17225 (2011).
24. M. S. Arnold, A. A. Green, J. F. Hulvat, S. I. Stupp, M. C. Hersam, *Nat. Nanotechnol.* **1**, 60 (2006).
25. H. Liu, D. Nishide, T. Tanaka, H. Kataura, *Nat. Commun.* **2**, 309 (2011).
26. Q. Cao, J. A. Rogers, *Adv. Mater.* **21**, 29 (2009).
27. K. Hata *et al*., *Science* **306**, 1362 (2004).
28. K. Koziol *et al*., *Science* **318**, 1892 (2007); 10.1126/science.1147635.
29. D. N. Futaba *et al*., *Nat. Mater.* **5**, 987 (2006).
30. Y. Hayamizu *et al*., *Nat. Nanotechnol.* **3**, 289 (2008).
31. M. De Volder *et al*., *Adv. Mater.* **22**, 4384 (2010).
32. M. Zhang, K. R. Atkinson, R. H. Baughman, *Science* **306**, 1358 (2004).
33. K. L. Jiang, Q. Q. Li, S. S. Fan, *Nature* **419**, 801 (2002).
34. W. Bauhofer, J. Z. Kovacs, *Compos. Sci. Technol.* **69**, 1486 (2009).
35. T.-W. Chou, L. Gao, E. T. Thostenson, Z. Zhang, J.-H. Byun, *Compos. Sci. Technol.* **70**, 1 (2010).
36. F. H. Gojny, M. H. G. Wichmann, U. Kopke, B. Fiedler, K. Schulte, *Compos. Sci. Technol.* **64**, 2363 (2004).
37. J. Suhr, N. Koratkar, P. Keblinski, P. Ajayan, *Nat. Mater.* **4**, 134 (2005).
38. J. N. Coleman, U. Khan, W. J. Blau, Y. K. Gun'ko, *Carbon* **44**, 1624 (2006).
39. H. G. Chae, Y. H. Choi, M. L. Minus, S. Kumar, *Compos. Sci. Technol.* **69**, 406 (2009).
40. V. P. Veedu *et al*., *Nat. Mater.* **5**, 457 (2006).
41. E. J. Garcia, B. L. Wardle, A. J. Hart, N. Yamamoto, *Compos. Sci. Technol.* **68**, 2034 (2008).
42. M. D. Lima *et al*., *Science* **331**, 51 (2011).
43. N. Behabtu *et al*., *Science* **339**, 182 (2013).
44. S. R. Bakshi, A. Agarwal, *Carbon* **49**, 533 (2011).
45. T. Kashiwagi *et al*., *Nat. Mater.* **4**, 928 (2005).
46. A. Beigbeder *et al*., *Biofouling* **24**, 291 (2008).
47. Z. Wu *et al*., *Science* **305**, 1273 (2004).
48. S. De, J. N. Coleman, *MRS Bull.* **36**, 774 (2011).
49. A. M. Ionescu, H. Riel, *Nature* **479**, 329 (2011).
50. S. J. Tans, A. R. M. Verschueren, C. Dekker, *Nature* **393**, 49 (1998).
51. J. Appenzeller, Y. M. Lin, J. Knoch, P. Avouris, *Phys. Rev. Lett.* **93**, 196805 (2004).
52. K. Jensen, J. Weldon, H. Garcia, A. Zettl, *Nano Lett.* **7**, 3508 (2007).
53. A. D. Franklin *et al*., *Nano Lett.* **12**, 758 (2012).
54. Q. Cao *et al*., *Nature* **454**, 495 (2008).
55. H. Park *et al*., *Nat. Nanotechnol.* **7**, 787 (2012).
56. D. M. Sun *et al*., *Nat. Nanotechnol.* **6**, 156 (2011).
57. M. A. McCarthy *et al*., *Science* **332**, 570 (2011).
58. P. Chen *et al*., *Nano Lett.* **11**, 5301 (2011).
59. M. Jung *et al*., *IEEE Trans. Electron. Dev.* **57**, 571 (2010).
60. M. C. LeMieux *et al*., *Science* **321**, 101 (2008).
61. A. D. Franklin *et al*., *ACS Nano* **6**, 1109 (2012).
62. M. H. van der Veen *et al*., paper presented at the 2012 IEEE International Interconnect Technology Conference, San Jose, CA, 4 to 6 June 2012.
63. T. Rueckes *et al*., *Science* **289**, 94 (2000).
64. L. Dai, D. W. Chang, J.-B. Baek, W. Lu, *Small* **8**, 1130 (2012).
65. A. R. Köhler, C. Som, A. Helland, F. Gottschalk, *J. Clean. Prod.* **16**, 927 (2008).
66. K. Evanoff *et al*., *Adv. Mater.* **24**, 533 (2012).
67. C. Sotowa *et al*., *ChemSusChem* **1**, 911 (2008).
68. Y. Gogotsi, P. Simon, *Science* **334**, 917 (2011).
69. A. Izadi-Najafabadi *et al*., *Adv. Mater.* **22**, E235 (2010).
70. T. Matsumoto *et al*., *Chem. Commun.* **2004**, 840 (2004).
71. A. Le Goff *et al*., *Science* **326**, 1384 (2009).
72. N. M. Gabor, Z. Zhong, K. Bosnick, J. Park, P. L. McEuen, *Science* **325**, 1367 (2009).
73. G. Gao, C. D. Vecitis, *Environ. Sci. Technol.* **45**, 9726 (2011).
74. M. S. Rahaman, C. D. Vecitis, M. Elimelech, *Environ. Sci. Technol.* **46**, 1556 (2012).
75. J. K. Holt *et al*., *Science* **312**, 1034 (2006).
76. B. Corry, *J. Phys. Chem. B* **112**, 1427 (2008).
77. D. A. Heller, S. Baik, T. E. Eurell, M. S. Strano, *Adv. Mater.* **17**, 2793 (2005).
78. A. De La Zerda *et al*., *Nat. Nanotechnol.* **3**, 557 (2008).
79. N. W. S. Kam, M. O'Connell, J. A. Wisdom, H. J. Dai, *Proc. Natl. Acad. Sci. U.S.A.* **102**, 11600 (2005).
80. T. Kurkina, A. Vlandas, A. Ahmad, K. Kern, K. Balasubramanian, *Angew. Chem. Int. Ed.* **50**, 3710 (2011).
81. D. A. Heller *et al*., *Nat. Nanotechnol.* **4**, 114 (2009).
82. E. S. Snow, F. K. Perkins, E. J. Houser, S. C. Badescu, T. L. Reinecke, *Science* **307**, 1942 (2005).
83. Z. Chen *et al*., *Nat. Biotechnol.* **26**, 1285 (2008).
84. A. Star *et al*., *Proc. Natl. Acad. Sci. U.S.A.* **103**, 921 (2006).
85. B. Esser, J. M. Schnorr, T. M. Swager, *Angew. Chem. Int. Ed.* **51**, 5752 (2012).
86. X. Shi, A. von dem Bussche, R. H. Hurt, A. B. Kane, H. Gao, *Nat. Nanotechnol.* **6**, 714 (2011).
87. S. Y. Hong *et al*., *Nat. Mater.* **9**, 485 (2010).
88. Z. Liu, X. Sun, N. Nakayama-Ratchford, H. Dai, *ACS Nano* **1**, 50 (2007).
89. A. Bianco, K. Kostarelos, M. Prato, *Chem. Commun.* **47**, 10182 (2011).
90. C. A. Poland *et al*., *Nat. Nanotechnol.* **3**, 423 (2008).
91. G. M. Mutlu *et al*., *Nano Lett.* **10**, 1664 (2010).
92. D. A. X. Nayagam *et al*., *Small* **7**, 1035 (2011).
93. E. W. Keefer, B. R. Botterman, M. I. Romero, A. F. Rossi, G. W. Gross, *Nat. Nanotechnol.* **3**, 434 (2008).
94. M. Endo, S. Koyama, Y. Matsuda, T. Hayashi, Y. A. Kim, *Nano Lett.* **5**, 101 (2005).
95. J. Pauluhn, *Regul. Toxicol. Pharmacol.* **57**, 78 (2010).
96. S. W. Hong *et al*., *Adv. Mater.* **23**, 3821 (2011).
97. K. H. Kim, Y. Oh, M. F. Islam, *Nat. Nanotechnol.* **7**, 562 (2012).

Acknowledgments: M.F.L.D.V. was supported by the Fund for Scientific Research–Flanders, Belgium. S.H.T. and A.J.H. were supported by the Office of Naval Research (N00014101055 and N000141210815). R.H.B. was supported by the Air Force Office of Scientific Research MURI grant R17535 and Robert A. Welch grant AT-0029. The authors thank M. Endo, Y. Gogotsi, K. Hata, S. Joshi, Y. A. Kim, E. Meshot, M. Roberts, S. Suematsu, K. Tamamitsu, J. R. Von Ehr, B. Wardle, G. Yushin, and many companies for valuable input.

Supplementary Materials

www.sciencemag.org/cgi/content/full/339/6119/535/DC1
Materials and Methods
Tables S1 to S3

10.1126/science.1222453